Research article

In vitro correction of cystic fibrosis epithelial cell lines by small fragment homologous replacement (SFHR) technique

Federica Sangiuolo[1], Emanuela Bruscia[1,2], Annalucia Serafino[3], Anna Maria Nardone[4], Emanuela Bonifazi[1], Monica Lais[1], Dieter C Gruenert[2] and Giuseppe Novelli*[1]

Address: [1]Department of Biopathology, Human Genetics Unit, Tor Vergata University of Rome, Italy, [2]Department of Medicine, Human Molecular Genetics Unit, University of Vermont, Burlington, VT, USA, [3]Institute of Experimental Medicine, CNR, Rome, Italy and [4]Azienda Ospedaliera Universitaria Policlinico Tor Vergata, Italy

E-mail: Federica Sangiuolo - sangiuolo@med.uniroma2.it; Emanuela Bruscia - emabruscia@yahoo.it; Annalucia Serafino - AnnaLucia.Serafino@ims.rm.cnr.it; Anna Nardone - anmnardone@hotmail.com; Emanuela Bonifazi - emanuela.bonifazi@yahoo.it; Monica Lais - moni_lais@hotmail.com; Dieter C Gruenert - dgruener@zoo.uvm.edu; Giuseppe Novelli* - novelli@med.uniroma2.it

*Corresponding author

Abstract

Background: SFHR (small fragment homologous replacement)-mediated targeting is a process that has been used to correct specific mutations in mammalian cells. This process involves both chemical and cellular factors that are not yet defined. To evaluate potential of this technique for gene therapy it is necessary to characterize gene transfer efficacy in terms of the transfection vehicle, the genetic target, and the cellular processing of the DNA and DNA-vehicle complex.

Methods: In this study, small fragments of genomic cystic fibrosis (CF) transmembrane conductance regulator (*CFTR*) DNA, that comprise the wild-type and ΔF508 sequences, were transfected into immortalized CF and normal airway epithelial cells, respectively. Homologous replacement was evaluated using PCR and sequence-based analyses of cellular DNA and RNA. Individual stages of cationic lipid-facilitated SFHR in cultured cell lines were also examined using transmission electron microscopy (TEM).

Results: We demonstrated that the lipid/DNA (+/-) ratio influences the mode of entry into the cell and therefore affects the efficacy of SFHR-mediated gene targeting. Lipid/DNA complexes with more negative ratios entered the cell via a plasma membrane fusion pathway. Transfer of the DNA that relies on an endocytic pathway appeared more effective at mediating SFHR. In addition, it was also clear that there is a correlation between the specific cell line transfected and the optimal lipid/DNA ratio.

Conclusions: These studies provide new insights into factors that underlie SFHR-mediated gene targeting efficacy and into the parameters that can be modulated for its optimization.

Background

Homologous replacement is a technology that can be used to modify specific genes within chromosomal DNA [1–6]. The potential of this type of strategy has obvious implications for maintaining genomic integrity and cell-specific expression. The direct conversion of mutant genomic sequences to a wild-type genotype, restoring the normal phenotype, has clear advantages over therapeutic cDNA. By preserving the integrity of the targeted gene, the relationship between the coding sequences and regulatory elements remains intact. Consequently, cell-specific expression is not altered. Small fragment homologous replacement (SFHR) involves the introduction of small fragments (~500-bp) of DNA into cells. After entering the cells, the fragment pairs with its genomic homologue and replaces the endogenous sequence with the exogenous fragment through an, as yet, undefined mechanism [1,2,6].

SFHR has already been successfully used to correct ΔF508 mutation in the cystic fibrosis (CF) transmembrane conductance regulator (*CFTR*) gene [1,2,7–10]. The ΔF508 is the most common mutation associated with CF [11,12] and demonstration of its correction has significant therapeutic implications. The studies showed that SFHR-mediated replacement of mutant or wild-type genomic sequences after the introduction of small DNA fragment (491/488 nt) into cultured epithelial cells [7,10]. In some studies, the fragment, also carried a silent mutation that introduced a unique *XhoI* restriction site that could be used as a secondary marker of SFHR-mediated correction [7,8].

Recent *in vivo* studies have also indicated that SFHR could be used to modify endogenous mouse *CFTR* in the lung and in the intestine [9]. Not only was it possible to demonstrate SFHR-mediated modification of the DNA, but there was also a clear indication that the cells expressing *CFTR* were modified [9]. However, there has been no detailed SFHR optimization analysis as it relates to the behaviour of the DNA during and after SFHR uptake, the intracellular distribution of the DNA, and long-term stability of SFHR using non-viral vehicles. In this study, different parameters that influence SFHR in human epithelial cells were evaluated to determine whether SFHR could be an effective strategy for gene therapy. These include the type of transfected cells, DNA fragment to lipid ratio (+/-, respectively) and the time of harvest after initiation of transfection (incubation time). Different DNA transfection conditions were evaluated with respect to their ability to modulate SFHR-mediated correction.

SFHR-mediated replacement at the appropriate genomic locus and expression of the exogenous sequences was assayed using polymerase chain reaction (PCR) amplification, restriction fragment length polymorphic (RFLP) analysis and DNA sequencing. The intracellular fate of transfected gold-labelled DNA fragments was monitored by transmission electron microscopy (TEM). The results presented here provide insight into the mechanisms underlying SFHR-mediated correction of the most common CF mutation, the ΔF508.

Methods

Cell cultures

Studies were carried out in CF tracheobronchial cells transformed with an origin of replication defective simian virus 40 (SV40) containing plasmid (pSVori-) [13–15]. The cell line, CFBE41o⁻, is homozygous for the ΔF508 mutation (ΔF508/ΔF508). A wild-type airway epithelial cell line 16HBE14o⁻, also transformed with the pSVori- plasmid was used as representative of the normal cells [14–16]. Cells were grown in Eagle's Minimal Essential Medium (MEM) supplemented with 10% fetal bovine serum (FBS) and antibiotics under humidified conditions at 37°C in 5% CO_2. Stock cultures were grown in T75 flasks coated with an extracellular matrix of collagen/fibronectin/bovine serum albumin and subculture by trypsinization as described previously [17].

Synthesis of DNA fragments

DNA fragments, 491-bp and 488-bp, that comprised exon 10 as well as the 3' and 5' flanking intron regions of the wild-type (wt) and mutant (ΔF508) *CFTR* gene respectively, were generated by PCR as previously described [7,8,10]. Fragments were column purified (Qiagen) and ethanol precipitated for subsequent use.

Preparation of lipid/fragment complexes

DNA-cationic lipid complexes were generated using the *GENEPORTER* (Gene Therapy Systems, San Diego, USA) liposome. The complexes were made at different charge ratios (+/-), by increasing the concentration of the double stranded DNA fragments and mixing with a constant quantity of *LIPID* (22.5 μl) according to manufacturer's specifications. The mixture was then incubated at room temperature for 45 min and diluted to a final volume of 2 ml with serum-free MEM. DNA without lipid was used as the control in all experiments.

Transfection protocol

Approximately 2.5×10^6 cells were seeded in T75 flask 24 h before treatment. Cells were incubated with lipoplexes for 5 h in serum free medium at 37°C. After the initial 5 h incubation, cell cultures were supplemented with medium containing a final 10% FBS concentration. Cells were harvested by trypsinization following removal of the culture medium and washing twice with cold Phosphate Buffered Saline (PBS).

Table 1: PCR primers for SFHR DNA and RNA analysis

Primer	Sequence	Location
CF1B (S)	5'-CCTTCTCTGTGAACCTCTATCA-3'	Intron 9
CF6 (A)	5'-CCACATATCACTATATGCATGC-3'	Intron 10
CF17 (S)	5'-GAGGGATTTGGGGAATTATTTG-3'	Intron 9
CF22 (A)	5'-CTTGCTAAAGAAATTCTTGCTC-3'	Intron 11
ΔF1 (S)	5'-TCCTGGATTATGCCTGGCACC-3'	Exon 10
ΔF2 (A)	5'-GGCATGCTTTGATGACGCTTC-3'	Exon 10

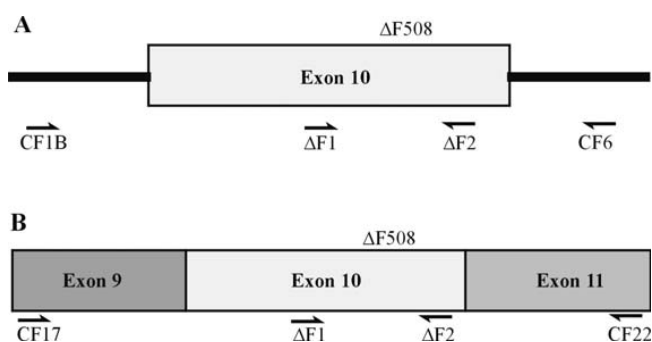Primer sequences are reported from ref. [7]

Figure 1
Localisation of primer pairs used for DNA (A) and RNA (B) analysis protocols. ΔF508 position is showed. PCR products length is of 771/768-bp, 373/370-bp and 97/94-bp for CF1B/CF6, CF1B/ΔF2 and ΔF1/ΔF2 oligonucleotide pairs respectively.

DNA analysis
Genomic DNA from transfected cells was initially PCR amplified with primers (CF1B/CF6) located outside the region of homology defined by the 491/488 bp transfection fragment (Fig. 1A). These primers localize the amplification to genomic DNA and inhibit amplification of free fragment. A secondary amplification was carried out with primers CF1B and ΔF2 with the primary amplification product as template. Primer ΔF2 is located inside the region of homology. A schematic representation of primer localization is depicted in Fig 1A. The product from the secondary PCR amplification was extracted from agarose gel (Millipore Ultrafree-DA, Bedford MA USA) and then subjected to a final round of radioactive PCR amplification with primers (ΔF1/ΔF2). These PCR products were sized by polyacrylamide gel electrophoresis (Storm 860, Molecular Dynamics, Little Chalfout, UK). The gel was exposed autoradiographically and then analyzed densitometricly to compare the relative intensity of the two bands (97 and 94 bp). These two bands correspond to the wild-type and mutant sequence, respectively. Oligonucleotide sequences are reported in Table 1I.

RNA analysis
Total RNA was extracted by using RNeasy Mini kit (Qiagen, Germany). Reverse Transcriptase PCR (RT-PCR) amplification of total RNA was carried out using Superscipt™ II RNAse H- Reverse Transcriptase (Gibco BRL Life Technologies, Gaithersburg, USA) to generate first strand cDNA. The cDNA was initially amplified with primers external from the homology region (CF17/CF22) and then with primers (CF17/ΔF2) (Fig. 1B). The PCR product from this secondary amplification was extracted from the agarose gel as above and subjected to a final round of PCR amplification with primers (ΔF1/ΔF2). The amplicons were sized and analysed by densitometric analysis. Results are presented as the standard error of the mean. Oligonucleotide sequences are reported in Table 1I.

Transmission electron microscopy analysis (TEM) of gold-labelled DNA fragments
DNA fragments were gold-labelled with photoactive biotin (Pierce, Illinois, USA), and Auroprobe EM streptavidin G10 (Amersham, United Kingdom), as previously described [13]. The CFBE41o- and 16HBE14o- cells were transfected with different amounts of labelled DNA/ lipid complex at varying charge ratios and analyzed at different times of transfection. Gold-labelled fragments (not complexed with lipid) were also transfected as controls. Cells were fixed for 1 hour at 4°C with 2.5% glutheraldheyde in 0.1 M Millonig's phosphate buffer (MPB) containing 2% sucrose. Samples were then post-fixed for 1 hour at 4°C with 1% OsO_4 in MPB, dehydrated in ascending ethanol concentrations and embedded in Spurr epoxy resin (Agar Scientific LTD, Stanted, Essex, UK). Ultrathin sections were stained with uranyl acetate and lead citrate and observed under a Philips CM12 transmission electron microscope (Philips, Philips Electronics, NV).

Results
Correction efficiency as function of lipid to DNA charge ratio (+/-): DNA analysis
The lipid/DNA ratios, based on charge ratio, were optimized using gel electrophoresis [18–20]. Complete neu-
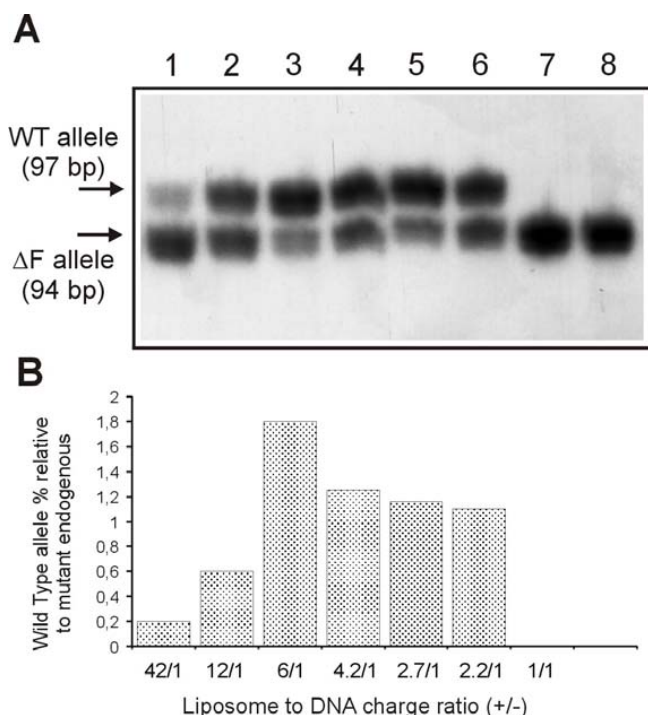
Figure 2
DNA analysis performed on CFBE41o⁻ transfected cells harvested 120 hrs after transfection. (A) PCR analysis of wild-type (WT) and ΔF508 alleles as a function of lipid to DNA charge ratios in CFBE41o⁻ cells. Replacement was indicated by the presence of the WT-allele for lipid/DNA ratios ranging from 42+/1- to 1+/1- corresponding to lanes from 1 to 7. DNA from untrasfected cells was amplified in lane 8 as negative control; (B) Densitometric analysis revealed that the maximum correction efficiency is reached with a ratio of lipid/DNA 6+/1-. No correction was observed at 1+/1- ratio.
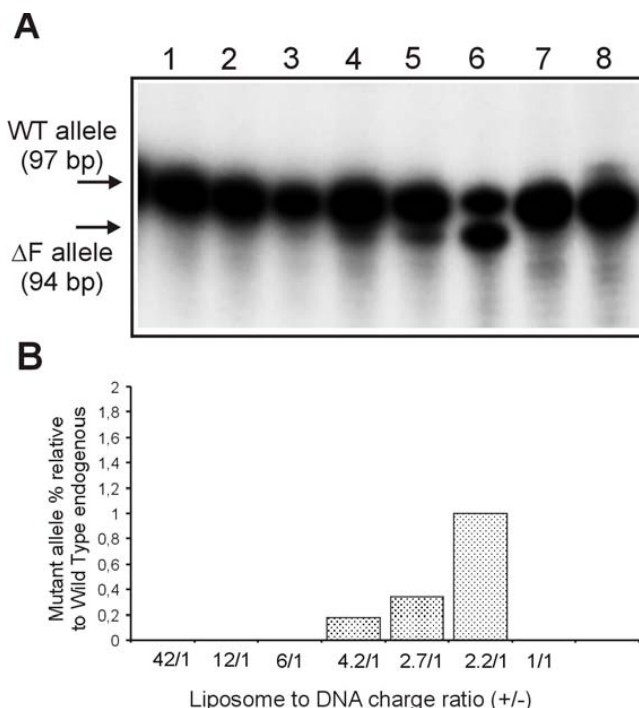

Figure 3
Analysis of DNA from 16HBE14o⁻ transfected cells. (A) PCR analysis of wild-type (WT) and ΔF508 alleles as a function of lipid to DNA charge ratios in 16HBE14o⁻ cells transfected with the ΔF508 DNA fragment. Replacement was indicated by the presence of the ΔF-allele after transfection at lipid to DNA ratios ranging from 42+/1- to 1+/1- (lanes from 1 to 7). DNA from untrasfected cells was amplified in lane 8 as negative control; (B) Densitometric analysis revealed that the maximum correction efficiency is reached with a lipid/DNA ratio of 2.2+/1-. With this cell line no correction was observed at ratios of 42+/1-, 12+/1-, 6+/1-and 1+/1-.

tralization of the negative DNA charge was achieved at a lipid to DNA charge ratio (+/-) of 2.2/1. A number of different lipid/DNA ratios were used to transfect (ΔF508/ΔF508) CFBE41o⁻ cells with wild-type 491 bp fragment. Fig. 2A shows allele-specific PCR analysis as a function varying the lipid/DNA ratio. A faint 97-bp amplification product, corresponding to the wild-type allele was evident at the highest lipid/DNA ratio. A more intense wild-type specific band was detectable up to 2.2+/1- ratio. The autoradiographic signal of the 97-bp band increased in intensity as the amount of DNA fragment in the lipid/DNA complex increased. Consequently, the overall charge of the lipid/DNA complex became less positive. However, when the charge of the complex was neutral, i.e. 1+/1-, the wild-type was not detectable. Densitometric analysis indicates that the relative signal of the wild-type band was maximal at a lipid /DNA charge ratio of 6+/1- (Fig. 2B). Thus, it appears the optimal Gene Porter/DNA fragment charge ratio of 6+/1- for SFHR-mediated replacement of ΔF508-*CFTR* in CFBE41o- cells.

SFHR-mediated gene modification was further characterised in wild-type cells (16HBE14o⁻) transfected with the ΔF508-*CFTR* DNA fragment (488-bp) in a lipid complex as described above. The subsequent PCR and radiographic analysis of the wild-type and ΔF508-*CFTR* alleles is presented in Fig. 3. A faint 94-bp, ΔF508-specific, amplification product could be detected at lipid/DNA charge ratio of 4.2+/1-. However, the 94-bp band with the greatest relative intensity was observed at a lipid/DNA ratio of 2.2+/1-. Densitometric analysis indicated that the amount of wild-type and ΔF508 product were equivalent (Fig. 3B). This result was supported by allele specific reverse-dot blot analysis of *CFTR* exon 10 (data not shown).

Correction efficiency as function of lipid to DNA charge ratio (+/-): RNA analysis
CFBE41o⁻ cells showed expression of the normal allele in a pattern similar to that observed for the relative DNA levels of the wild-type allele (Fig. 4A). However, the SFHR-
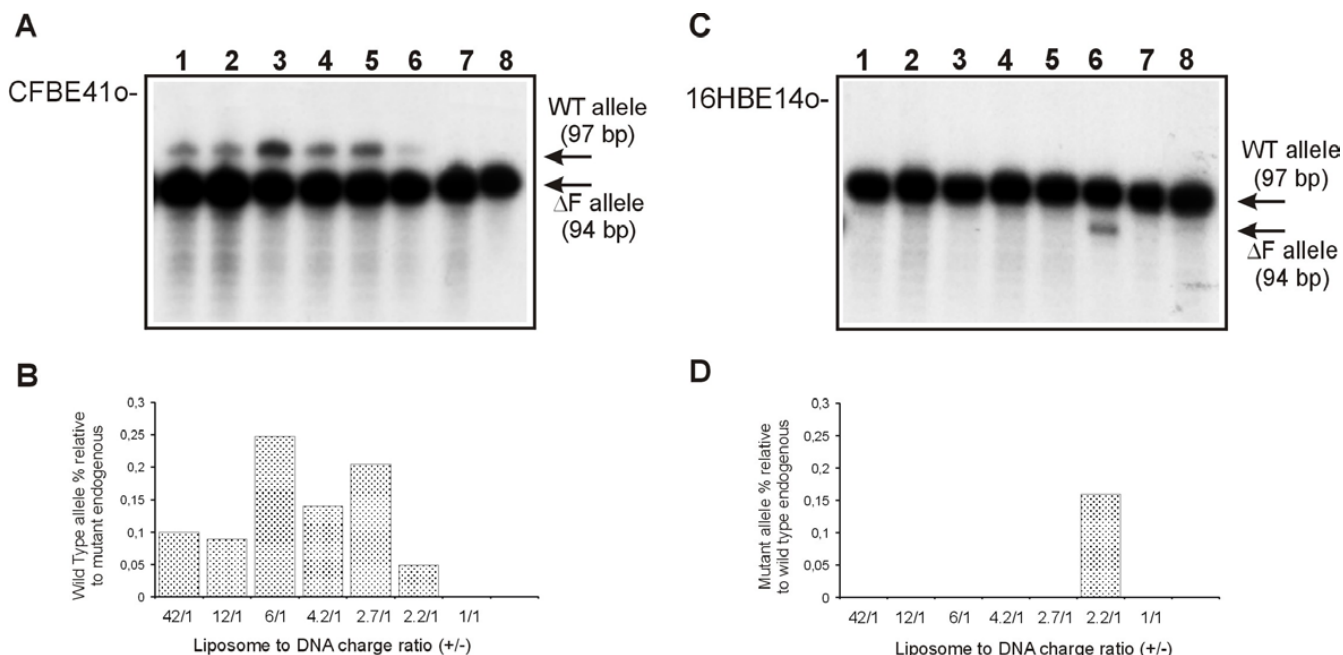
Figure 4
Analysis of RNA from CFBE41o⁻ (A, B) and 16HBE14o⁻ (C, D) transfected cells at different lipid/DNA ratios and harvested 120 hrs after transfection. Lanes 1-7 correspond to lipid/DNA charge ratios ranging from 42+/1- to 1+/1-. Lane 8 is RNA analysis of untransfected cells (A, C). The expression of the recombinant allele was detected in lanes 1 to 6 in (A) and in lane 6 only in (C). Densitometric analysis revealed that the maximum correction efficiency in CFBE41o⁻ is reached with a lipid/DNA ratio of 6+/1- (B), whereas in 16HBE14o⁻ recombinant allele is expressed only at 2.2/1 charge ratio (+/-) as reported in (D).

modified wild-type allele is expressed at the levels much lower than the endogenous mutant allele (ΔF508), as shown by densitometric analysis revealing that the maximum correction efficiency in CFBE41o⁻ is reached with a lipid/DNA ratio of 6+/1- (Fig. 4B).

Similar results were obtained for the 16HBE14o⁻ cells transfected with the ΔF508 DNA fragment (Fig. 4C). Transcription of the ΔF508 mutant allele was only detectable at a lipid/DNA ratio of 2.2+/1- (Fig. 4C/D), corresponding to the maximum correction efficiency observable in genomic DNA (Fig. 3A/B).

Analysis of targeted replacement at different times after transfection with small DNA fragments
The stability of the SFHR-mediated exchange after exposure to the lipoplexes was evaluated to determine the effective detectability of SFHR-mediated homologous replacement as a function of time. Cells were transfected at the optimal lipid/DNA charge ratio for each cell line (6+/1- and 2.2+/1- for CFBE41o- and 16HBE14o-, respectively) and harvested at 24 h, 48 h, 72 h, 96 h and 120 h after termination of the lipoplex incubation. Analysis of the DNA from transfected CFBE41o- cells indicates the greatest degree of SFHR-mediated replacement 24 h after transfection (Fig. 5A). SFHR-mediated homologous re-

placement continued to be detectable up to 11 days post transfection in CFBE41o- cell (data not shown). No apparent signal was detected when cells were harvested at 16, 21, and 30 days following transfection (data not shown). It has to be noted that the intensity values between densitometric analysis results in fig 2B (lane 3) and fig. 5B (lane 5) are different. The experiments were repeatead twice and the results come out from arithmetic mean. These results could be explained by the polyploid status of the cell line used for transfections. Thus, the fragment can recombine in more *CFTR* loci. The highest level of SFHR-mediated exchange in 16HBE14o- cells was observed at 48 h and then again at 120 h post transfection (Fig. 5B).

TEM analysis of lipoplex-cell interactions
The intracellular route that the DNA fragments take to traffic to the cell nucleus was monitored using TEM and lipid/gold-labelled DNA complexes at different charge ratios (+/-). Cells were fixed and observed at different times after the start of transfection ranging from 5 h to 96 h (Fig. 6,7,8,9). In cells treated at the optimal lipid/DNA charge ratio complexes (6+/1-), an endocytotic-like pattern of internalization was observed (Fig. 6B,6C). Nevertheless, DNA/lipid complexes were never observed in coated pits,
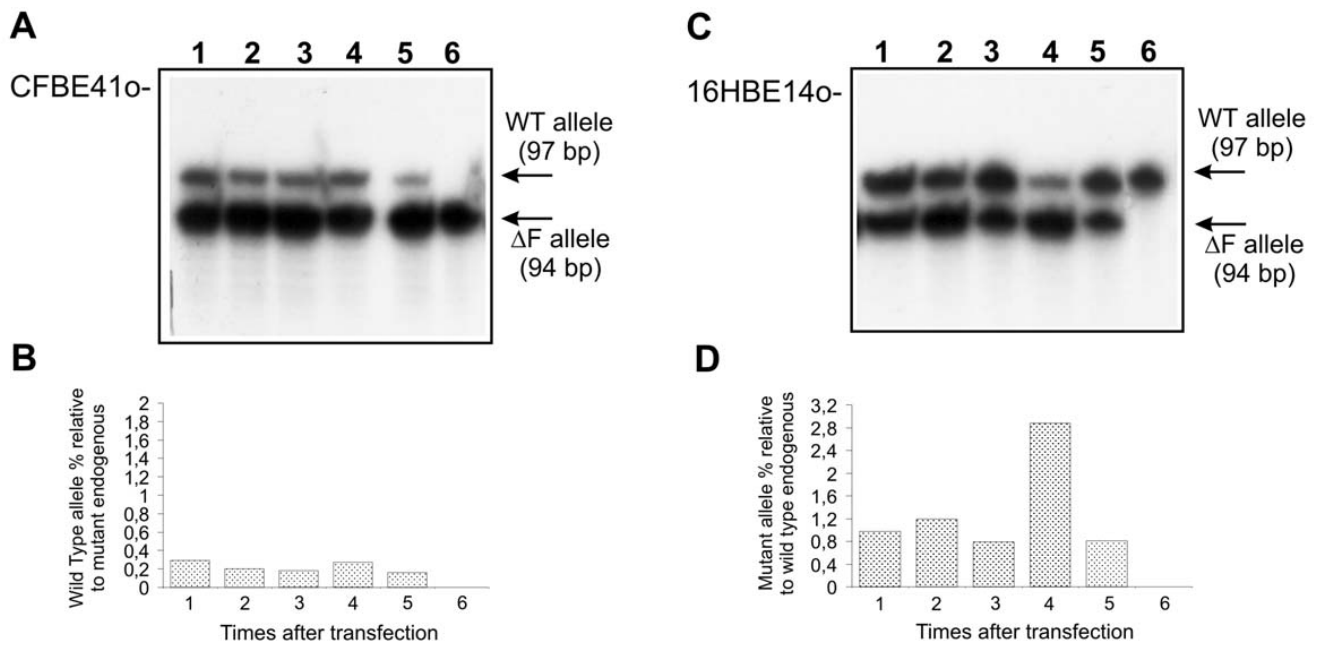
Figure 5
Analysis of DNA from CFBE41o⁻ (A) and 16HBE14o⁻ (C) transfected cells at optimal lipid/DNA charge ratio (6+/1- and 2.2+/1-respectively) and harvested at 24 h (lane1), 48 h (lane2), 72 h (lane 3), 96 h (lane 4) and 120 h (lane 5) after transfection. Lane 6 corresponds to untransfected cells. Densitometric analysis revealed that the maximum correction efficiency in CFBE41o⁻ is reached at 24 h after transfection (B), while in 16HBE14o⁻ at 48 h and again at 120 h after transfection (D).
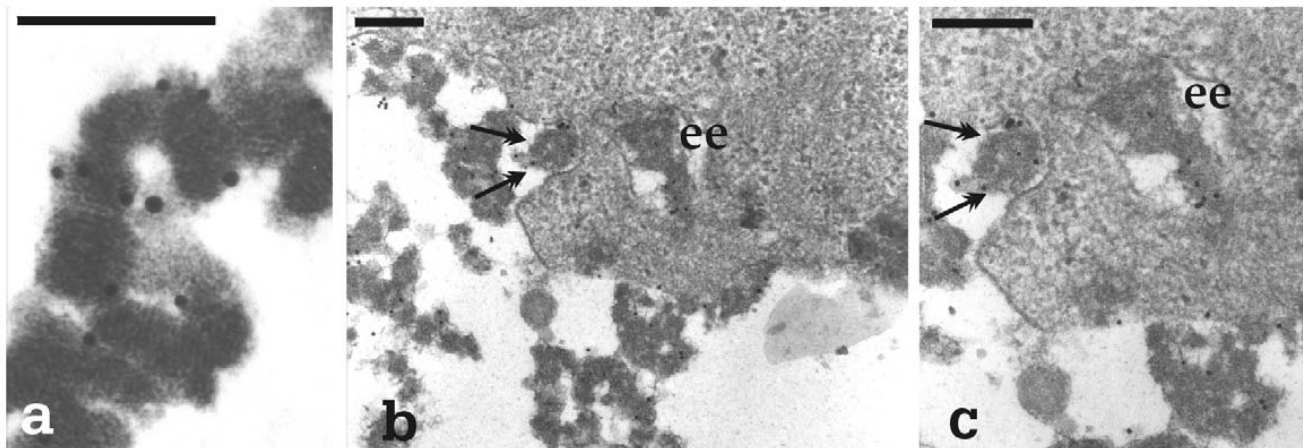

Figure 6
Transmission EM of CFBE41o⁻ cells transfected at the optimal lipid/DNA ratio (6+/1-) and fixed 5 h after the start of transfection. (A) gold-labelled DNA complex; (B) labelled complexes interacting with cell membrane; (C) a detail of B at higher magnification. ee: early endosome. Arrows indicate endocytosis of the lipid/DNA complex. Bars: 200 nm.
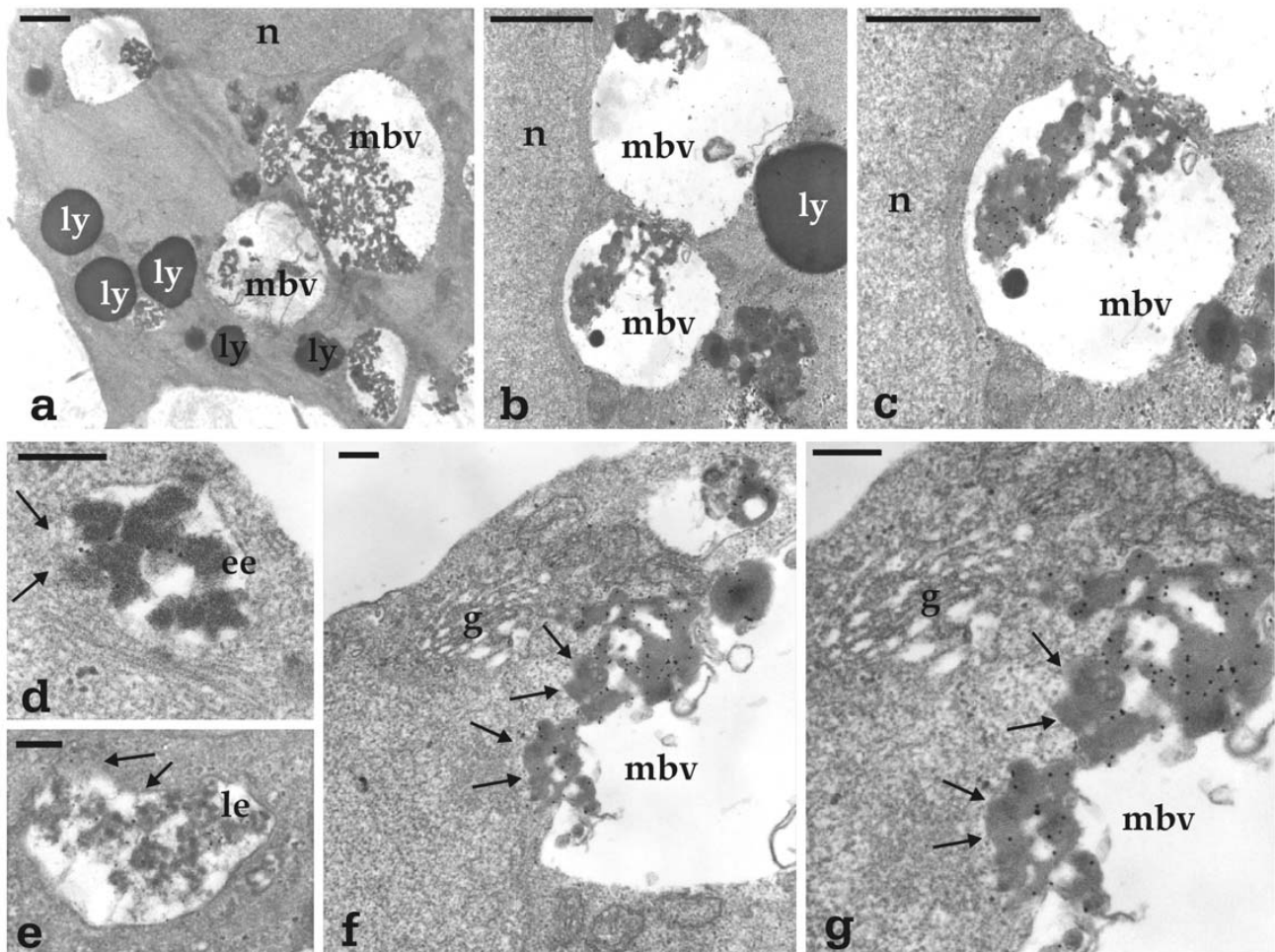
Figure 7
Transmission EM of CFBE41o⁻ cells transfected at the optimal lipid/DNA ratio (6+/1-) and fixed 72 h after the start of transfection. (A)-(C) large membrane-bound vesicles containing aggregates of labelled complexes in the perinuclear region of transfected cells. Destabilization of an early endosome (D), late endosome (E) and membrane-bound vesicles (F and G) by lipid/DNA complexes; (G) a higher magnification of (F). Arrows indicate a part of the aggregated complexes extruded into the cytoplasm and not surrounded by an endosome or a large vesicle membrane. ee: early endosome; g: Golgi apparatus; le: late endosome; mbv: membrane-bound vesicle; ly: lysosome; n: nucleus. Bars: (A)-(C): 1 µm; (D)-(G)): 200 nm.

suggesting that the internalization of the complexes was not achieved through receptor-mediated endocytosis (Fig 6B,6C).

The complexes appeared as structures around gold-labelled DNA (Fig. 6A). Some endosomes containing the complexes were near the cell surface suggesting that these were early endosomes (Fig. 6C). With an increase in the time of exposure to the transfection complexes, the endosomes appeared to move towards the perinuclear region. Late endosomes fused together to generate large membrane-bound vesicles containing aggregates of labelled complexes (Fig 7A,7B,7C). As shown in Fig. 7D,7E,7F,7G the DNA lipid complexes seemed to destabilize both en-

dosomes and large membrane-bound vesicles. It should be noted that the destabilization site along the progression of the endosome to large vesicle seemed to be preferentially near the Golgi apparatus and the vesicular compartment of endoplasmic reticulum (Fig 7F,7G). These observations suggest that the DNA-liposomes complexes might be released into the cytoplasm by destabilizing either the endosome and large vesicle membrane and that the endoplasmic reticulum may be involved in the transport of free DNA towards the nucleus. Occasionally, gold labelled electron-dense material, apparently not bound to liposome structures, was observed near the ER and near the nuclear pores (data not shown). Free gold labelling was never observed in the nucleus. This may be
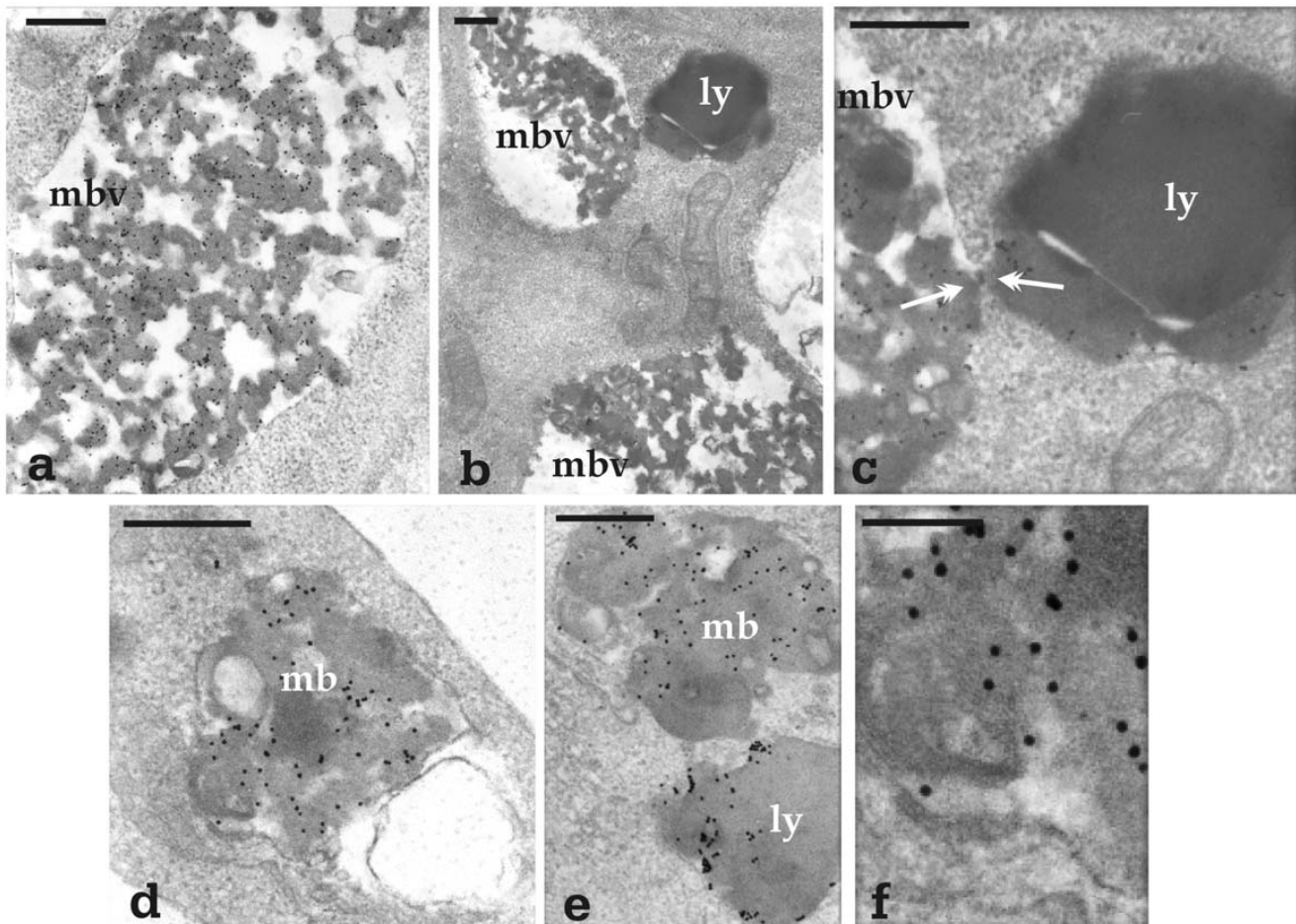
Figure 8
Transmission EM of CFBE41o⁻ cells transfected at the (6+/1-) lipid/DNA ratio and fixed 96 h after the start of transfection. (A)-(C) Large vesicles filled with labelled complexes in the cytoplasm of a transfected cell; (C) a higher magnification of (B). Arrows indicate a fusion site between a large vesicle and a lysosome. (D)-(F) labelled membranous body and lysosome in the cytoplasm of a transfected cell; (F) a higher magnification of a membranous body, in which the lipid/DNA complexes appeared partially degraded. ly: lysosome; mb: membranous body; mbv: membrane-bound vesicles. Bars: (A)-(E): 300 nm; (F): 100 nm.

due to the fact that, because of the size of the DNA fragments, not all the DNA was gold labeled. Consequently, our inability to observe free gold labeled DNA in the nucleus might reflect that very little DNA (gold labeled and unlabeled) escaped from the endosome and that the sensitivity of electron microscopy is not high enough to detect it. Alternatively, it is possible that, during the delivery of the DNA fragments from the complexes, some of the gold labelling was removed. At 96 hrs after the start of transfection, very large vesicles filled with gold-labelled complexes were observed (Fig 8A,8B,8C). Furthermore, large membranous bodies showing a regular lamellar pattern, similar to those described previously [21], were frequently observed (Fig 8D,8E). Of note is that the multilamellar packed structure of complexes that was still visible in the large cytoplasmic vesicles (Fig 8C), whereas

in the large membranous bodies and apparent lysosomes the liposome complexes were not distinguishable (Fig 8E,8F). One possible explanation for this observation is that continued cellular exposure to the liposomes/DNA complexes results in their accumulation in large cytoplasmic vesicles. When the complexes in these vesicles exceed a critical concentration, the vesicles could neither fuse with lysosomes (Fig. 8C) and result in degradation of the complexes inside the large membranous bodies.

TEM analysis of cells treated with lipid/ DNA ratios that showed no SFHR-mediated modification showed labelled complexes adhering to the cytoplasmic membrane of a small number of cells (Fig. 9A). These complexes were never observed inside endosomes. Furthermore, in some cases the adherent complexes seemed to destabilize, the
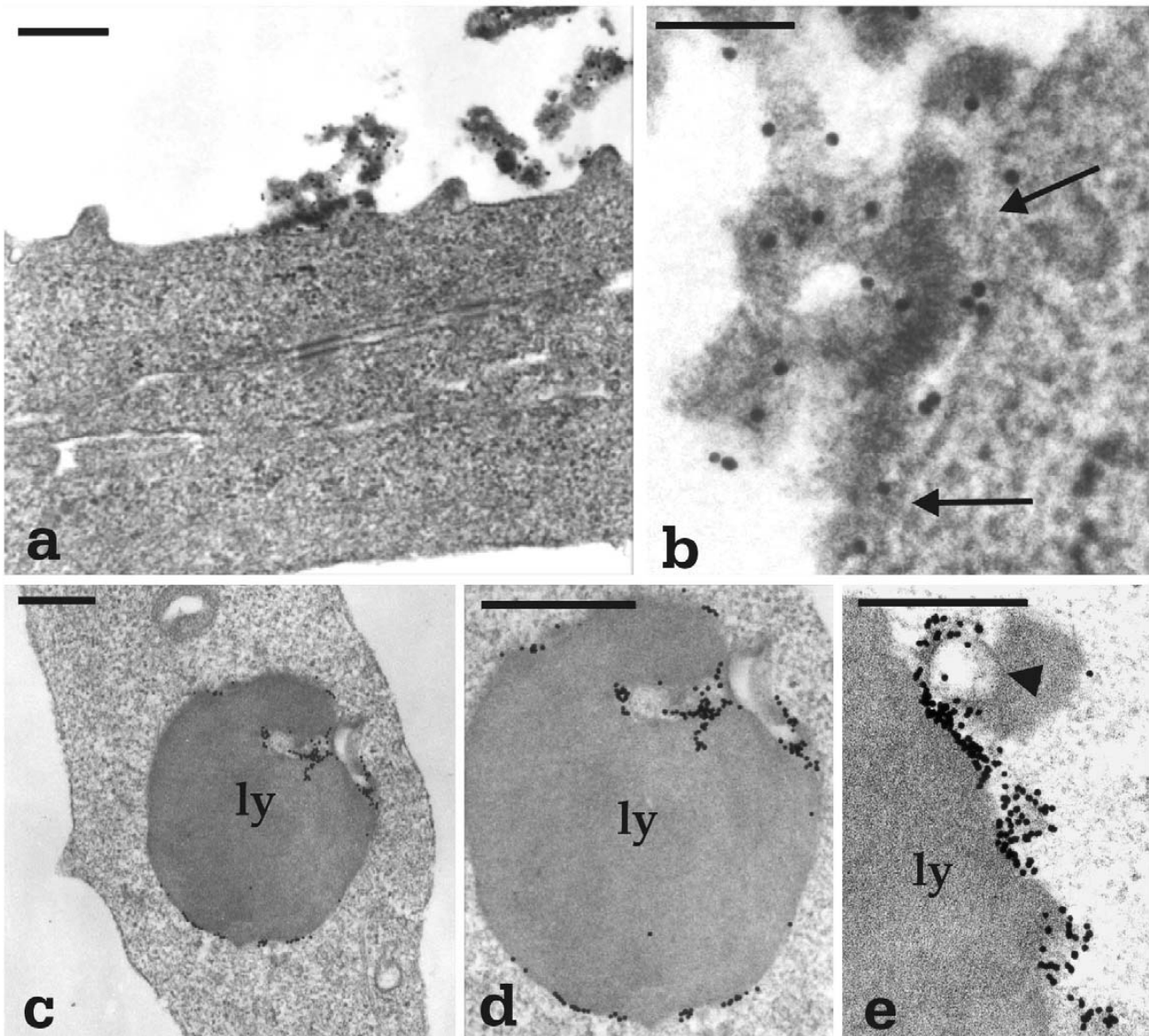
Figure 9
Transmission EM of CFBE41o⁻ cells transfected at a lipid/DNA ratio having no transfection activity (1+/1-). Cells were fixed at 5 h (A and B) and at 72 h (C and E) after the start of transfection. (A) and (B) show labelled complexes adhering to the cellular membrane; (B) is a higher magnification of (A). Arrows indicate sites at the plasma membrane that appear to be destabilised by the adhering complex. (C)-(E) show a labelled lysosome in a transfected cell; (E) is at high magnification. In (E) the lipid/DNA complexes, adhering to the lysosome membrane, appear to be free within the cytoplasm (*arrowhead*). ly: lysosome. Bars: (A), (C), (D), (E): 300 nm; (B): 100 nm.

cell membrane (arrows in Fig. 9B). Both observations suggest that these lipid/DNA complexes penetrated the cell by a fusion mechanism. At these charge ratios, gold labelling was observed almost exclusively around and inside lysosomes (Fig. 9C,9D), and labelled complexes were never observed in late endosomes or large vesicles. These observations suggest that when lipid/DNA complexes enter the cell via a fusion mechanism, they are immediately digested by lysosomes. Thus, the entry of lipid/DNA complexes via an endocytic mechanism seems to be a requirement for the release of the DNA from the lipoplexes and transport into the nucleus. Controls were monitored in which labelled fragments, not complexed with lipid, were transfected for testing labelling toxicity. No fragments were seen inside cells (data not shown).

Discussion

SFHR-mediated gene targeting has been used to correct a specific *CFTR* mutation, in the 3-bp ΔF508 deletion [7,10]. Recently, this strategy was successfully employed to correct a nonsense mutation in the dystrophin (*dys*) locus of the *mdx* mouse both *in vitro* and *in vivo*[22]. Previous studies have also shown that DNA fragments can be delivered to the lung by lipid vehicles. In this study, SFHR-mediated correction was detected up to seven days at mRNA level within lung and lower airways, suggesting its therapeutic potential within this organ [9].

These previous studies results suggest that SFHR has therapeutic potential for treatment of inherited disorders. However, to enhance this therapeutic potential, transfection conditions need to be optimized. This can, in part, be achieved by analysis of the cellular and molecular mechanisms that underlie transport of the therapeutic fragments to the nucleus. One of the necessary conditions to achieve therapeutically relevant SFHR-repair efficiencies is a careful optimization of delivery methodologies to overcome both extracellular and intracellular barriers that preclude the nuclear localization of the small fragments.

In fact, a major hurdle of gene therapy is the limited nuclear uptake of intact therapeutic DNA that inhibits its full performance [21].

The lipid/DNA ratio appears to be an important factor influencing the success of transfection [18,23,24]. The results of the studies presented here indicate that the lipid/DNA charge ratios for optimal SFHR-mediated modification are cell line dependent. A molar charge ratio of 2.2 (+)/1(-) and 6 (+)/1(-) for the wild-type (16HBE14o-) and the mutant (CFBE41o-) cell lines, respectively, was found to be optimal for SFHR when assessed by PCR. When the amount of lipid was held constant and the amount of DNA was increased, a more negatively charged lipid/DNA complex was formed. While increasing the

amount of DNA in the lipoplexes, SFHR-mediated modification was observed to progressively decrease until it was undetectable (up to 30 µg of fragment). These findings indicate that the amount of DNA is not rate limiting in itself, but rather that the reduction in positive charge caused by an increase in DNA within the lipoplexes, impacts SFHR-mediated modification. This effect on SFHR was clearly cell line dependent and appears to be associated with the transport of the DNA to the nucleus. Alternatively, it can not be ruled out that the increased amount of DNA in negatively charge lipid/DNA complexes might competitively inhibit the enzymatic processes that leads to DNA uptake and/or SFHR. If the enzymatic pathways are saturated with DNA fragments they might not be as effective at mediating exchange. This will require further analysis in a future study.

Knowledge of the internalization mechanism and intracellular fate of lipoplexes is a prerequisite for the further development of efficient SFHR-based gene repair protocols. TEM analysis demonstrated that the lipoplexes enter cells via different mechanisms that depend on the lipid/DNA charge ratio. At a more negative charge ratio, lipoplexes enter into cells via a fusion pathway. Complexes that enter the cell via fusion with the plasma membrane appear not to enter the nucleus to mediate SFHR as is implied by the apparent lack of correction detected by molecular analysis. These results are consistent with previous work investigating the role of helper lipid in the assembly [18] and destabilization [23] of lipoplexes, and in the finding that lipid can inhibit SFHR-mediated modification of mutant plasmids after transient transfection [24].

The TEM analysis also demonstrated that lipoplexes with the appropriate charge could be taken up in endosomes within 5 h after initiation of transfection and become associated with the nucleus within 72 h. This endocytic uptake mechanism for the lipoplex appears to be distinct from that involving fusion with the plasma membrane, but also dependent on the lipoplex charge. As the lipoplex molar charge ratio becomes more positively charged, the lipoplexes appear to enter the cells via an endocytic pathway. It is this pathway that appears to be more effective at transferring DNA to the nucleus and mediating SFHR. Therefore, strategies that enhance endosome disruption might further improve delivery to the nucleus and thus potentiate SFHR-mediated modification. These include incorporation of synthetic virus-derived "fusogen" into the lipid complex [25,26], the introduction of membrane destabilizing peptides into DNA/poly-lysine conjugates [27], transfection in the presence of inactivated adenovirus [28,29] as well as treatment of the cells with agents that enhance endosome lysis such as chloroquine and glycerol [30–32].

SFHR-mediated DNA modification was detected within the population of transfected cells for at least 120 hours post-transfection. Analysis of the transfected CFBE41o-cells showed the 3-bp insertion at 11 days post-transfection. However, at 30 days, the insertion was no longer apparent. Recent studies in which the mixed population of transfected cells was sorted into isogenic cell lines have indicated that subpopulations of corrected cells exist within the larger population, albeit at a frequency that is detectable by allele-specific PCR [33]. Thus, it does appear that SFHR-mediated modification of CFBE41o- cells is stable over time, but the proportion of corrected cell is reduced, leading to dilution of the signal because of the passing of time.

Conclusions

These studies demonstrate that the efficacy of lipid assisted SFHR-mediated modification appears to be cell line-dependent. Different charge ratios were optimal for SFHR-mediated targeting when comparing CFBE41o⁻ cells to 16HBE14o⁻ cells. This suggests that, as yet undefined, intracellular factors influence lipid-facilitated SFHR-mediated modification. The data are also consistent with previous observations that the efficiency of cationic lipid-mediated transfection varies with different cell types [18,34,35]. This issue will be particularly relevant to the selection of the delivery vehicles for SFHR *in vitro* and *in vivo*[9,22].

While recent studies demonstrated that SFHR delivery can be achieved *in vivo* in the mouse lung [9] and muscle [22], there are still questions that need to be answered before SFHR can be applied therapeutically. Although it is difficult to extrapolate conditions and optimal delivery vehicle formulations from *in vitro* experiments to *in vivo*, these studies on human airway epithelial cell lines provide insights into therapeutic application of SFHR in human airways. In the context of a reliable assay system these cell systems, can be useful for elucidating those conditions that will optimize SFHR in the airways [18,24].

Competing interests
None declared.

Authors' contributions
F.S., M.L., E.B. and E.B. carried out molecular genetic studies, A.N. carried out cell cultures, A.S. carried out TEM analysis, D.G. participated in the design of the study and G.N. conceived the study, and participated in its coordination.

All authors read and approved the final manuscript.

Acknowledgements

References

1. Gruenert DC: **Gene correction with small DNA fragments.** *Curr Res Molec Ther* 1998, **1**:607-613
2. Gruenert DC: **Opportunities and challenges in targeting genes for therapy.** *Gene Ther* 1999, **6**:1347-1348
3. Kmiec EB: **Targeted gene repair.** *Gene Ther* 1999, **6**:1-3
4. Lai LW, Lien YH: **Homologous recombination based gene therapy.** *Exp Nephr* 1999, **7**:11-14
5. Woolf TM: **Therapeutic repair of mutated nucleic acid sequences.** *Nat Biotechnol* 1998, **16**:341-344
6. Yanez RJ, Porter ACG: **Therapeutic gene targeting.** *Gene Ther* 1998, **5**:149-159
7. Goncz KK, Kunzelmann K, Xu Z, Gruenert DC: **Targeted replacement of normal and mutant *CFTR* sequences in human airway epithelial cells using DNA fragments.** *Hum Mol Genet* 1998, **7**:1913-1919
8. Goncz KK, Gruenert DC: **Site-directed alteration of DNA by small fragment homologous replacement (SFHR).** *In: Gene Targeting Vector Protocols (Edited by: Kmiec EB, Totowa NJ) Humana Press* 1998, 85-99
9. Goncz KK, Colosimo A, Dallapiccola B, Gagne L, Hong K, Novelli G, D Papahadjopoulos, Sawa T, Schreier H, Wiener-Kronish J, *et al*: **Expression of ΔF508 *CFTR* in normal mouse lung after site-specific modification of *CFTR* sequences by SFHR.** *Gene Ther* 2001, **8**:961-965
10. Kunzelmann K, Legendre JK, Knoell D, Escobar LC, Xu Z, Gruenert DC: **Gene Targeting of *CFTR* DNA in CF epithelial cells.** *Gene Ther* 1996, **3**:859-867
11. Kerem B, Rommens JM, Buchanan JA, Markiewicz D, Cox TK, Chakravarti A, Buchwald M, Tsui LC: **Identification of the cystic fibrosis gene: genetic analysis.** *Science* 1989, **245**:1073-1080
12. Tsui LC: **The spectrum of cystic fibrosis mutations.** *Trends in Genet* 1992, **8**:392-398
13. Cozens AL, Yezzi MJ, Chin L, Simon EM, Finkbeiner WE, Wagner JA, Gruenert DC: **Characterization of immortal cystic fibrosis tracheobronchial gland epithelial cells.** *Proc Natl Acad Sci USA* 1992, **89**:5171-5175
14. Gruenert DC, Basbaum CB, Welsh MJ, Li M, Finkbeiner WE, Nadel JA: **Characterisation of human tracheal epithelial cells transformed by an origin-defective simian virus 40.** *Proc Natl Acad Sci USA* 1988, **85**:5951-5955
15. Gruenert DC, Finkbeiner WE, Widdicombe JH: **Culture and transformation of human airway epithelial cells.** *Am J Physiol* 1995, **268**:L347-360
16. Cozens AL, Yezzi MJ, Kunzelmann K, Ohrui T, Chin L, Eng K, Finkbeiner WE, Widdicombe JH, Gruenert DC: ***CFTR* expression and chloride secretion in polarized immortal human bronchial epithelial cells.** *Am J Respir Cell Mol Biol* 1994, **10**:38-47
17. Gruenert DC, Basbaum CB, Widdicombe JH: **Long-term culture of normal and cystic fibrosis epithelial cells grown under serum-free conditions.** *In Vitro Cell Dev Biol* 1990, **26**:411-418
18. Colosimo A, Goncz KK, Holmes AR, Kunzelmann K, Novelli G, Malone RW, Benneth MJ, Gruenert DC: **Transfer and expression of foreign genes in mammalian cells.** *Biotechniques* 2000, **29**:314-318
19. Densomore CL, Giddings TH, Waldrep JC, Kinsey BM, Knight V: **Gene transfer by guanidinium-cholesterol-dioleoylphosphatidyl-ethanolamine liposome-DNA complexes in aerosol.** *J Gene Med* 1999, **1**:251-264
20. Felgner PL: **Nonviral strategies for gene therapy.** *Sci Am* 1997, **276**:102-106
21. Zabner J, Fasbender AJ, Moninger T, Poellinger KA, Welsh MJ: **Cellular and molecular barriers to gene transfer by a cationic liposome.** *J Biol Chem* 1995, **270**:18997-19007
22. Kapsa R, Quigley A, Lynch GS, Steeper K, Kornberg AJ, Gregorevic P, Austin L, Byrne E: ***In vivo* and *in vitro* correction of the mdx dystrophin gene nonsense mutation by short-fragment homologous replacement.** *Hum Gene Ther* 2001, **12**:29-642
23. Colosimo A, Sangiuolo F, Di Sario S, Amicucci P, Serafino AL, Novelli A, Sabati M, Castro M, Lucidi V, Mossa G, Dalla piccola B, Novelli G: **Current status of cationic liposome-mediated gene therapy in cystic fibrosis.** *Acta Pharm* 1998, **4**:221-227

24. Colosimo A, Goncz KK, Novelli G, Dallapiccola B, Gruenert DC: **Targeted correction of a defective selectable marker gene in human epithelial cells by small DNA fragments.** *Mol Ther* 2001, **3:**178-185

25. Scheule RK, Bagley RG, Erickson AL, Wang KX, Fang SL, Vaccaro C, O'Riordan CR, Cheng SH, Smith AE: **Delivery of purified, functional *CFTR* to epithelial cells in vitro using influenza hemagglutinin.** *Am J Respir Cell Mol Biol* 1995, **13:**330-343

26. Schreier H, Ausborn M, Gunther S, Weissig V, Chander R: **(Patho)physiologic pathways to drug targeting: artificial viral envelopes.** *J Mol Recognit* 1995, **8:**59-62

27. Schwarzenberg P, Huang W, Oliver P, Osidipe T, Theodossiou C, Kolls JK: **Poly-L-Lisine based molecular conjugate vectors: a high efficiency gene transfer system for human progenitor and leukemia cells.** *Am J Med Sci* 2001, **321:**129-136

28. Kafri T: **Lentivirus vectors: difficulties and hopes before clinical trials.** *Curr Opin Mol Ther* 2001, **3:**316-26

29. Evans JT, Cravens P, Gatlin J, Kelly PF, Lipsky PE, Garcia JV: **Pre-clinical evaluation of an in vitro selection protocol for the enrichment of transduced CD34(+) cell-derived human dendritic cells.** *Gene Ther* 2001, **8:**1427-35

30. Remy-Kristensen A, Clamme JP, Vuilleumier C, Kuhry JG, Mely Y: **Role of endocytosis in the transfection of L929 fibroblasts by polyethylenimine/DNA complexes.** *Biochim Biophys Acta* 2001, **1514:**21-32

31. Ma H, Diamnond SL: **Nonviral gene therapy and its delivery systems.** *Curr Pharm Biotechnol* 2001, **2:**1-17

32. Nishikawa M, Huang L: **Nonviral vectors in the new millennium: delivery barriers in gene transfer.** *Hum Gene Ther* 2001, **12:**861-70

33. Bruscia E, Sangiuolo F, Goncz KK, Novelli G, Gruenert DC: **Isolation of CF cell lines corrected at ΔF508-*CFTR* locus by SFHR-mediated targeting.** *Gene Ther* 2002

34. Caplen NJ, Kinrade E, Sorgi F, Gao X, Gruenert DC, Geddes D, Coutelle C, Huang L, Alton EW, Williamson R: ***In vitro* liposome-mediated DNA transfection of epithelial cell lines using the cationic liposome DC-Chol/DOPE.** *Gene Ther* 1995, **2:**603-613

35. Gao XA, Huang LA: **A novel cationic liposome reagent for efficient transfection of mammalian cells.** *Biochem Biophys Res Commun* 1991, **179:**280-285

Pre-publication history

The pre-publication history for this paper can be accessed here:

http://www.biomedcentral.com/1471-2350/3/8/prepub